

Article

Computational Modeling of the Feasibility of Substituted [1.1.1]Propellane Formation from Anionic Bridgehead Bromide Precursors

Katherine E. Gates, Caitlin Herring, Andrew T. Lumpkin, Robert J. Maraski, Elizabeth G. Perry, Madelen G. Prado, Sarah L. Quigley, Jazmine V. Ridlehoover, Edith Salazar, Kynslei Sims, Kaitlin R. Stephenson, Emma A. Stewart, Mackenzie E. Sullivan, James R. Tucker  and Gary W. Breton * 

Department of Chemistry and Biochemistry, Berry College, 2277 Martha Berry HWY, Mount Berry, GA 30149, USA

* Correspondence: gbreton@berry.edu

Abstract: [1.1.1]Propellane, a compound whose structure includes two saturated carbons in which all four bonds are directed into a single hemisphere, is of theoretical interest, but has also seen recent practical applications. Mono-, di-, and trisubstituted derivatives of this propellane (by substitution of its CH₂ bridges with O, S, NH, CF₂, CO, SO, and SO₂) remain unknown despite several computational studies that have suggested some may be stable. In this study, we show that, in several cases, substituted propellanes are spontaneously formed upon the attempted computational optimization of the geometries of anionic bridgehead bromide precursors using the ωB97X-D/aug-cc-pVDZ DFT method. Spontaneous formation suggests that these propellanes are at lower energy relative to the precursors and, therefore, are promising synthetic targets. The success or failure to spontaneously form the propellane is considered in relation to the length and strain energy of the central bridgehead-bridgehead bond, as well as the total strain energy of each propellane.

Keywords: propellanes; [1.1.1]propellane; optimization; strained bonds



Citation: Gates, K.E.; Herring, C.; Lumpkin, A.T.; Maraski, R.J.; Perry, E.G.; Prado, M.G.; Quigley, S.L.; Ridlehoover, J.V.; Salazar, E.; Sims, K.; et al. Computational Modeling of the Feasibility of Substituted [1.1.1]Propellane Formation from Anionic Bridgehead Bromide Precursors. *Organics* **2023**, *4*, 196–205. <https://doi.org/10.3390/org4020016>

Academic Editor: Edward Lee-Ruff

Received: 27 March 2023

Revised: 14 April 2023

Accepted: 23 April 2023

Published: 4 May 2023



Copyright: © 2023 by the authors. Licensee MDPI, Basel, Switzerland. This article is an open access article distributed under the terms and conditions of the Creative Commons Attribution (CC BY) license (<https://creativecommons.org/licenses/by/4.0/>).

1. Introduction

[1.1.1]Propellane, **1** (Figure 1), a compound whose structure includes two saturated carbons in which all four bonds are directed into a single hemisphere, was first synthesized in 1982 by Wiberg [1]. While **1** remains a target of fascination for theoretical chemists because of the unusual bonding arrangement between the two inverted bridgehead carbons [2–5], it has also seen recent practical applications for a variety of synthetic purposes [6,7]. There has been ongoing interest in the possibility of synthesizing mono-, di-, and trisubstituted [1.1.1]propellanes by replacing one or more of the CH₂ groups of **1** (see compounds **2–4**, Figure 1) [8–16]. Although these substituted compounds remain synthetically elusive, several computational studies have suggested the possibility that they could exist as stable entities [8,10,12,13]. A computational study on a series of trisubstituted propellanes, **4**, was carried out by Pittman using a coupled-cluster approach (CCSD/aug-cc-pVDZ) [8]. That study identified a number of trisubstituted [1.1.1]propellanes that appeared to be sufficiently stable so as to recommend them as synthetic targets.

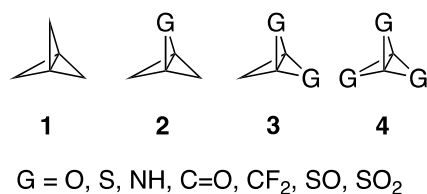
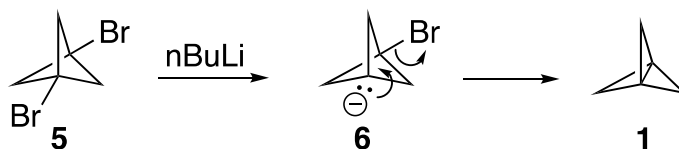


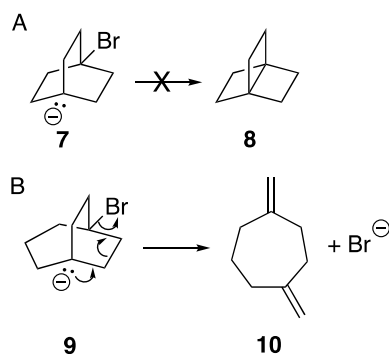
Figure 1. Structure of the parent [1.1.1]propellane (**1**), and variously substituted analogs **2–4**.

Wiberg's synthesis of [1.1.1]propellane is outlined in Scheme 1 [1]. Thus, upon treating 1,3-dibromobicyclopentane, **5**, with $n\text{BuLi}$, a metal/halogen exchange process occurs that leads to the formation of the anionic bridgehead bromide intermediate **6**. The intramolecular displacement of the second bromine atom forms the strained bridgehead-bridgehead bond. A number of other propellanes have been synthesized in a similar manner [17,18], which provides a straightforward and perhaps general means by which to synthesize propellanes, including (potentially) those substituted as discussed above.



Scheme 1. Formation of [1.1.1]propellane (**1**) via formation of anionic bridgehead bromide **6** by way of the 1,3-dibromobicyclopentane, **5**.

In an earlier computational study, we found that, upon an attempted computational optimization of the geometry of the unsubstituted anionic bridgehead bromide compound **6** at the B3LYP/6-31G* level of theory, it spontaneously formed **1** via an ejection of the bridgehead bromine as a bromide ion during the optimization process [19]. Thus, compound **6** itself was not a stationary point on the potential energy surface (PES) but led seamlessly to the propellane structure, thereby mimicking the experimental behavior observed by Wiberg. Furthermore, we were able to successfully model a number of other spontaneous formations of propellanes from anionic bridgehead bromide compounds that varied by the number of carbon atoms in the bridges [19]. Interestingly, however, attempts at forming the [2.2.2]propellane **8** (see Scheme 2) via an optimization of anionic bridgehead bromide **7** was unsuccessful, with the central bridgehead-bridgehead bond resisting formation [19]. This computational behavior appeared to portend the experimental finding that [2.2.2]propellane, formed in a manner similar to that outlined in Scheme 1, is highly unstable, and unable to be isolated. Additionally, optimizing the geometry of the [3.2.2] anionic bridgehead bromide **9** resulted in the loss of the bromine atom as a bromide ion, but with bond scission (i.e., a Grob fragmentation) to form the bis-methylene compound **10** rather than the formation of the propellane [19]. Interestingly, a similar Grob fragmentation process had been observed as the means of decomposition of **8** as well as several other propellanes [17,20]. While [3.2.2]propellane has been synthesized and characterized [21], it was not synthesized via an anionic bridgehead precursor, so it is not known whether it would undergo a Grob fragmentation under those reaction conditions. Overall, then, it appeared that computational modeling did a remarkable job of predicting known experimental results.



Scheme 2. (A) Anionic bridgehead bromide **7** fails to form [2.2.2]propellane **8** upon geometry optimization. (B) Optimization of **9** leads to fragmentation to form **10** instead of a propellane.

In Pittman's study, the feasibility of formation of the substituted propellanes **4** was based solely on the anticipated strain energies of the final propellane structures [8]. Modeling the final propellane product may indicate whether the propellane has any chance of

existing or not, but it provides no indication as to whether there is an energetic driving force for the formation of the central bond. The computational optimizations discussed above provide this information, as either the central bond will be formed, or not, depending on whether the propellane is at lower energy relative to the anionic bridgehead bromide, and as long as there is a viable energetic pathway that allows for its formation. If such a viable energetic path exists, we would expect spontaneous ejection of the bromine as a leaving group and the formation of the substituted propellane upon geometry optimization. The synthetic pursuit of these substituted [1.1.1]propellanes would, therefore, be most promising. If a viable energetic path does not exist, we would expect that either the anionic bridgehead bromide would optimize as a stationary point of its own (i.e., it does not lead to propellane formation), or another pathway may be followed other than that of the propellane formation (e.g., such as Grob fragmentation). These substituted propellanes would either not be attractive to pursue synthetically (especially if the strain energies of the propellane structures themselves are particularly high), or they should be pursued using a synthetic method other than via anionic bridgehead bromide precursors.

In the current study, we have modeled a series of anionic bridgehead bromides substituted at one, two, and all three of the bridging CH₂ groups of **6** to observe whether they would spontaneously form the corresponding propellanes upon optimization. We chose many of the same groups as earlier investigated by Pittman to allow for direct comparison with those findings. In addition, we have analyzed the strain energies inherent in all of the proposed propellanes and have attempted to correlate the strain energies with the propensity to form propellanes upon geometry optimization of the precursor anions. Based upon this work, we are able to recommend pursuing the synthesis of those propellanes most likely to be successfully formed via the synthetic method outlined in Scheme 1.

2. Materials and Methods

All the calculations were performed at the ω B97X-D/aug-cc-pVDZ level of theory in the solvent THF via the polarizable continuum model (PCM) using the software package GAMESS [22,23] as implemented through the ChemCompute.org website [24]. Default computational parameters were employed. All the optimizations were repeated at least three times to ensure the consistency of the results. The frequency calculations were carried out at all stationary points to ensure the lack of imaginary frequencies.

3. Results and Discussion

Pittman selected the CCSD computational level of theory for modeling a series of substituted [1.1.1]propellanes **4** [8]. Unfortunately, however, this level of theory is exceedingly time and resource expensive, especially when using it to model the (often) many iterative steps required to eject the bromide ion from the anionic bridgehead bromides to form the resulting substituted [1.1.1]propellanes. We had used density functional theory (DFT) successfully in our earlier work [19], and we decided to continue using DFT. However, we opted to switch from the B3LYP functional we had used earlier to the more robust ω B97X-D functional, which provides the benefit of including dispersion effects that are absent in B3LYP but could be of importance during the geometry optimizations [25]. Additionally, the ω B97X-D functional has been used in a number of recent studies by others to successfully describe the reactivity of propellanes and related structures [26–28]. We used the same basis set (aug-cc-pVDZ) as employed by Pittman as it includes diffuse functions that are important for the accurate modeling of anions. Furthermore, this basis set is of a size sufficient to model these compounds (as reflected by Pittman's work), but it is not so large as to make the calculations unwieldy. Finally, we included solvent effects using the polarizable continuum model (PCM) to better reflect the behavior of the ions in solution. Tetrahydrofuran (THF) was selected as a solvent since it is a solvent often chosen for synthetic work with carbanions. All stationary points were tested by calculating the IR frequencies to confirm the absence of any imaginary frequencies.

While Pittman and others have focused on [1.1.1]propellanes substituted at all three of the bridging CH₂ groups, we have expanded these studies to investigate the effect of mono- (**2**), di- (**3**), and trisubstitution (**4**) of the CH₂ bridges of **1**. This allows for understanding the cumulative effect of successive substitution and may indicate whether lesser-substituted propellanes (i.e., **2** and **3**) might be more viable synthetic targets than the fully substituted counterparts (i.e., **4**).

3.1. Comparison of Computational Methods for Modeling Propellanes 1–4

We began by optimizing the geometries of the neutral substituted propellanes in comparison with previous results by Pittman, where available. In general, the bridgehead-bridgehead bond distances are calculated to be slightly shorter than those calculated using the CCSD method, with the mean absolute difference being 0.037 Å (see column 2, Table 1). The CCSD method predicted an order of $4\text{O} < 4\text{NH} < 4\text{S} < 4\text{CH}_2 < 4\text{CF}_2 < 4\text{SO} < 4\text{SO}_2$ for the propellane bond lengths [8]. The results of the $\omega\text{B97X-D}$ method are in good agreement with the CCSD results, with the exception of a swap between 4CF_2 and 4SO . However, these two bond lengths are predicted to be close to one another according to both of the computational methods (1.721 and 1.733 for CCSD, respectively, and 1.698 and 1.697 for $\omega\text{B97X-D}$). Additionally, the bond length values calculated in this work were nearly identical to several of the same bond lengths calculated at the B3LYP/6-31G(d,p) level of theory as reported earlier [11]. Interestingly, the DFT method did not locate 4CO as a stationary point. Instead, repeated attempts at optimizing to the corresponding propellane led to ring opening to form bisketene **11** (Figure 2). Note, however, that the bond length predicted when using the CCSD method for 4CO of 1.855 Å is exceptionally long, suggesting that 4CO as modeled using CCSD is not a true propellane structure to begin with, and likely occupies an unsustainable geometry. The same can be said for 4SO_2 for which CCSD predicted a bond length of 1.978 Å, and ωB97XD a bond length of 1.912 Å, both well out of the range of a possible legitimate C–C bond. On the whole, therefore, we were satisfied with the geometries predicted using the ωB97XD DFT functional in relation to those calculated using the CCSD method.

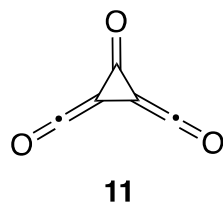


Figure 2. Structure of the bisketene obtained upon attempted optimization of 4CO .

3.2. Optimization of Anionic Bridgehead Bromide Precursors

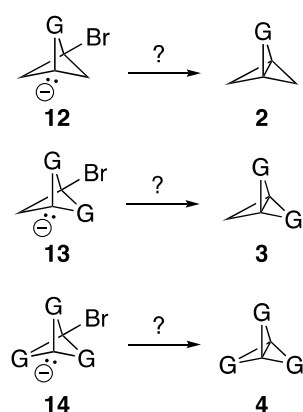
The geometries of the anionic bridgehead bromide compounds **12**, **13**, and **14** (see Scheme 3) were optimized at the $\omega\text{B97X-D}/\text{aug-cc-pVDZ}$ level of theory. Note that, for those compounds with multiple N–H bonds or S–O bonds, the H/O atoms were oriented so as to be in a uniform clockwise direction. In addition, while we used NH bonds to simplify the calculations, an N–H bond would be incompatible with the formation of bridgehead anions, and the use of N–R derivatives would be more practical (e.g., R = Me). For all the compounds, optimization led either to ejection of the Br atom as a bromide ion and formation of the corresponding propellane, or simple optimization of the originally guessed geometry for the anionic bridgehead bromide compounds. In no cases were ring-opened or alternative products formed. If propellane formation did not occur, a frequency calculation was carried out on the optimized anionic bridgehead bromide compounds to ensure that it was a stationary point at an energy minimum. The results of these optimizations are compiled in column 3 of Table 1. As representative examples of the outcomes of these optimizations, the result of the optimization of precursor **12O** that led successfully to propellane **2O** is shown in Figure 3A, and the optimization of precursor **14O** that did not

result in the formation of propellane **4O**, but only in the optimization of the geometry of **14O**, is shown in Figure 3B. A video showing the iterative steps involved in the optimization of precursor **12O** to form **2O** is provided in the Supplementary Materials.

Table 1. Summary of results on the length of the optimized propellane central bonds, calculated strain energies, and whether optimizations of the anionic bridgehead bromide precursors led to propellane formation.

Propellane	Propellane C–C Bond Distance ¹ (Å)	Propellane Formation Upon Optimization Of Precursor? ²	Propellane Total Strain E ³ (kcal/mol)	Propellane Central Bond Strain E ⁴ (kcal/mol)
1	1.566 (1.604)	Yes	“0”	“0”
2O	1.529	Yes	5	7
3O	1.500	Yes	11	21
4O	1.482 (1.511)	No	27 (18)	40
2NH	1.544	Yes	2	2
3NH	1.525	Yes	3	7
4NH	1.511 (1.537)	Yes	4 (–2)	13
2S	1.573	Yes	1	4
3S	1.573	Yes	3	6
4S	1.557 (1.601)	No	9 (3)	5
2CF₂	1.610	Yes	16	11
3CF₂	1.656	Yes	39	21
4CF₂	1.698 (1.721)	No	69 (61)	30
2CO	1.661	Yes	17	17
3CO	1.755	No	39	31
4CO	N/A ⁵ (1.855)	No	N/A ⁵ (57)	N/A ⁵
2SO	1.614	Yes	–4	10
3SO	1.660	No	1	16
4SO	1.697 (1.733)	No	11 (–2)	18
2SO₂	1.687	No	16	20
3SO₂	1.808	No	50	33
4SO₂	1.912 (1.978)	No	103 (82)	41

¹ The distance between the bridgehead carbons of the corresponding propellanes as modeled at ω B97X-D/aug-cc-pVDZ. Values in parenthesis correspond to Pittman’s distances calculated using the CCSD/aug-cc-pVDZ method [8]. ² “Yes” means the anionic bridgehead bromide formed the corresponding [1.1.1]propellane upon geometry optimization. “No” means a propellane failed to form. ³ Total strain energy of the propellane relative to unsubstituted **1** according to isodesmic Equations (1)–(3). Values in parenthesis correspond to values calculated in an identical manner by Pittman but using the CCSD/aug-cc-pVDZ method [8]. ⁴ Strain energy of the central bridgehead–bridgehead bond relative to unsubstituted **1** as calculated according to isodesmic Equations (4)–(6). ⁵ This [1.1.1]propellane was not a stationary point on the potential energy surface at the ω B97X-D/aug-cc-pVDZ level of theory.



Scheme 3. Anionic bridgehead bromide precursors **12–14** that were computationally optimized to see if they spontaneously converted to propellanes **2–4**.

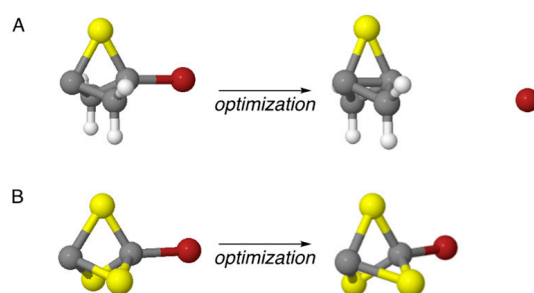


Figure 3. Representative results of optimizations for examples in which computational optimization of anionic bridgehead bromide precursor (A) **12O** led to formation of corresponding propellane **2O** via ejection of the bromine atom as bromide, and (B) **14O** did not lead to formation of propellane **4O** but only to optimization of the geometry of the precursor. Atom colors: gray= carbon; yellow = oxygen; and red = bromine.

Several general observations may be made from the data in the table:

- (i) In almost all cases, trisubstituted compounds **14** failed to generate the propellane **4**, with the exception of **14NH**.
- (ii) In no cases were propellanes formed at substitution levels beyond those in which propellane formation failed (i.e., if propellane formation failed for **3**, propellane formation also failed for **4**).
- (iii) The most resistant-to-form propellanes were those precursors substituted with CF_2 , CO , SO , and SO_2 groups.
- (iv) While there is no direct correlation between the bond length of the propellane central bond and whether the propellane formed or not, generally those with shorter bond distances ($<1.66 \text{ \AA}$) were more likely to successfully form, while those with longer bond distances ($>1.66 \text{ \AA}$) were resistant to forming.

For those anionic bridgehead bromide precursors that failed to form a propellane, we calculated the free energy change for the formation of the propellane from the corresponding anionic precursor. The results are provided in Table 2. For most cases (**4O**, **4S**, **4CF₂**, **3CO**, **4SO**, **3SO₂**, and **4SO₂**) the conversions are endergonic, which clearly explains the resistance to spontaneous formation of the propellane. However, for two of the cases (**3SO** and **2SO₂**), the conversions are exergonic. In these two cases, the lack of formation of the propellanes could possibly be attributed to the ability of these substituents to stabilize the negative charge on the precursor, thereby overcoming the energetic drive to form the corresponding propellanes.

Table 2. Free energy change for formation of propellanes from the corresponding anionic bridgehead bromide precursors.

Propellane	ΔG (kcal/mol) ¹
4O	+28
4S	+15
4CF₂	+7
3CO	+1
3SO	-5
4SO	+9
2SO₂	-8
3SO₂	+22
4SO₂	+40

¹ Difference in free energy between the optimized anionic bridgehead bromide precursor and the sum of the energies of the neutral propellane and Br^- .

From these observations, it would appear that anionic bridgehead bromides **12** and **13** substituted with O, NH, and S would be the most attractive synthetic targets with the highest likelihood of successfully forming the desired corresponding propellanes.

3.3. Estimating the Total Strain Energy in Propellanes 2–4

Pittman had utilized an isodesmic equation, represented by Equation (1) of Figure 4, to estimate the total strain energies inherent in the trisubstituted propellanes **4** relative to unsubstituted **1** [8]. We extended his method of calculating the strain energies for the mono and disubstituted derivatives **2** and **3** according to Equations (2) and (3). These calculated strain energies are provided in column 4 of Table 1.

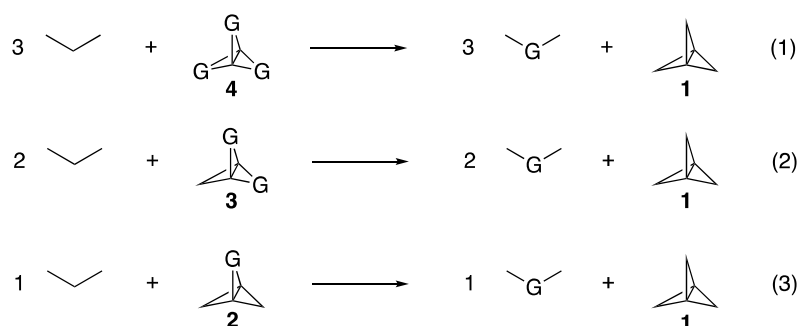


Figure 4. Pittman’s isodesmic equation to estimate the overall strain energy of trisubstituted propellanes **4** relative to unsubstituted **1** is represented by Equation (1) [8]. Extension of this methodology to the mono- and disubstituted propellanes **2** and **3** are represented by isodesmic Equations (2) and (3).

As can be seen in Table 1, while there is reasonable agreement between the relative total strain energies calculated at the ω B97X-D versus the CCSD levels of theory, the DFT method consistently provided slightly higher strain energy estimates relative to CCSD theory. However, the general trend of the relative energies is retained, and groups may be partitioned into those with low (4NH, 4S, and 4SO), medium (4O), and high (4CF₂, 4CO, and 4SO₂) levels of strain. Furthermore, there is generally observed to be an increase in the strain energy with each subsequent substitution of a CH₂ bridge as one progresses in the series from **2** to **4**. For NH, S, and SO substitutions, the increase in the strain energy upon successive substitution is relatively small. This is especially true for NH substitutions in which the strain energy increases only marginally with increasing substitution. For O, the third substitution to form **4O** dramatically increases the strain relative to **2O** and **3O**, but, overall, the strain is not very high. Particularly interesting, however, is the low strain energies predicted for the sulfoxide series. The propellane **2SO** is predicted to be even less strained than unsubstituted **1**, while **3SO** and **4SO** remain only marginally more strained. In contrast to those substituted series for which the strain is manageable, each addition of a CF₂, CO, or SO₂ group increases the strain energy dramatically.

As with the C–C bond distance of the final propellane structures, there is no obvious direct correlation of the probability of the successful formation of a propellane upon geometry optimization of an anionic bridgehead bromide with the total strain energy of the final propellane, although the propellane formation was generally favored when the total strain energy was less than 27 kcal/mol. However, several propellanes with strain energies below this level (e.g., **4S**, **3SO**, **4SO**, and **2SO**) also failed to spontaneously form.

3.4. Estimating the Central Bridgehead-Bridgehead Bond Strain Energy in Propellanes 1–4

Given that the total strain energy of the final propellanes was not a conclusive indicator as to whether the propellane would form spontaneously upon the optimization of the anionic bridgehead bromide precursor, we wondered whether a better predictor would be the strain energy of the centrally formed bridgehead-bridgehead bond. Isodesmic Equations (4)–(6) (see Figure 5) were developed to more directly isolate the strain experienced by the central propellane bonds of the derivatives relative to that of the unsubstituted

propellane **1**. The energies of the variously substituted bicyclopentanes found on the right side of these equations and the energy of the unsubstituted bicyclopentane found on the left side of these equations were calculated using the same optimization conditions as had been used for the propellanes. The resulting change in energy for each derivative was taken as an estimate of the strain energy localized at the bridgehead-bridgehead bond relative to that of **1**. These calculated central bond strain energies are compiled in column 5 of Table 1.

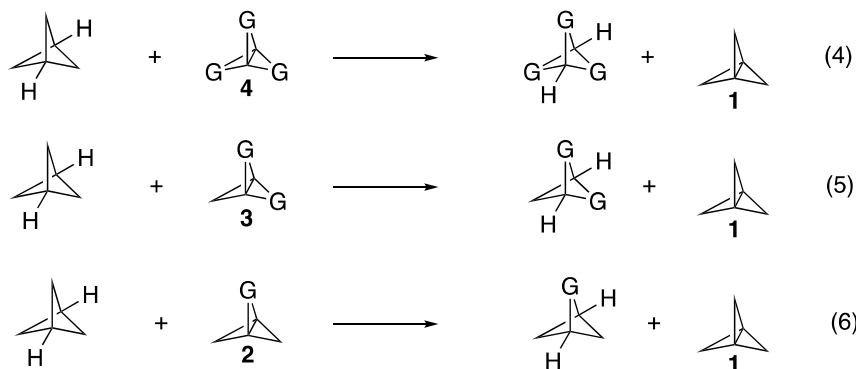


Figure 5. Isodesmic reactions to estimate the amount of strain energy present in the central bridgehead-bridgehead bonds of propellane derivatives **2–4** relative to unsubstituted **1**.

The trend in the strain energies of the central bonds calculated via isodesmic reactions (4)–(6) was identical to that calculated earlier on a subset of these compounds using the B3LYP/6-31G(d,p) method based on hydrogenation of the central bond of the propellane to form the corresponding bicyclopentane (see Equation (7) in Figure 6) [9,11]. Both methods predict the order of stability of **1** > 2NH > 2S ~ 3NH ~ 2O > 4NH > 3O > 4O.

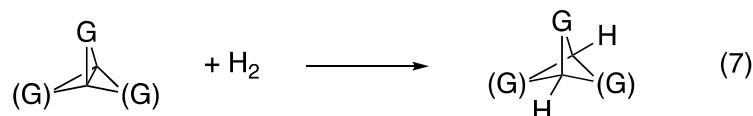


Figure 6. Estimation of strain on the central bond of a subset of the propellanes **2–4** based on the heat of hydrogenation as described in [9].

An interesting trend emerges when comparing the central bond energy strain (column 5, Table 1) relative to the total strain energies (column 4, Table 1). For those substituted propellanes that had overall lower total strain energies (O, NH, S, and SO), one notices that the strain of the central bond is generally higher than the total strain energy of the molecules. Hence, the central bond strain is compensated for by the substituents either structurally and/or electronically. However, for those propellanes that had higher total strain energies (CF₂, CO, and SO₂), their total strain energies are generally greater than that of the central bond strain energy. Hence, those substituents are unable to compensate for the strain introduced by the central bond and their bonding situation is apparently worsened either structurally and/or electronically. While it is certainly of interest as to what structural and/or electronic factors may be at play to either accommodate or exacerbate the strain energies of these molecules, this would require an in-depth analysis of the complex bonding situations [2], which is beyond the scope of this current work.

The central bond strain energies were, therefore, also not direct predictors as to whether the propellane structure would form spontaneously upon geometry optimization of **12–14**. While, generally, propellane formation occurred with compounds containing low central bond energy strain (i.e., <21 kcal/mol), in some cases, propellane formation failed to occur (e.g., for 4S, 3SO, 4SO, and 2SO₂). However, in no cases were propellanes formed when the central bond strain energy exceeded 21 kcal/mol.

4. Conclusions

In many of the studied cases, geometry optimization of the anionic bridgehead bromide precursors spontaneously formed the corresponding propellane compounds. This suggests that for those compounds, the propellane is energetically favored relative to the precursor, and has a higher likelihood of forming the propellane experimentally. It should be noted, however, that for those anionic bridgehead bromides that did not spontaneously form propellanes, it is not impossible that they could also successfully form propellanes under the proper conditions. It may be that those bromides have an energetic barrier toward the formation of the propellanes, and, when provided that energy, may be able to surmount that barrier and form the desired propellanes. However, in our quest to locate the most promising propellane targets, we prioritize the anionic bridgehead bromides that form the propellanes spontaneously upon optimization. Combining the results of the optimizations with what was learned from the analysis of the lengths of the central propellane bonds and the strain energies (both total strain energies and those of the central bond), it would appear that the most promising synthetic targets using the synthetic method outlined in Scheme 1 would be those propellanes that:

- (i) Successfully formed the corresponding propellane upon geometry optimization of precursors **12–14**.
- (ii) Form propellanes that have central bridgehead-bridgehead bond lengths $<1.66 \text{ \AA}$.
- (iii) Have low total strain energies (i.e., $<27 \text{ kcal/mol}$).
- (iv) Have low central C-C bond energies (i.e., $<21 \text{ kcal/mol}$).

The most synthetically attractive propellanes, therefore, would be compounds **2O**, **2NH**, **3NH**, **4NH**, **2S**, and **3S**. Compounds **2CF₂**, **2CO**, and **2SO** are also possible contenders, but the behavior of their more highly substituted counterparts render them more suspect than the former recommendations. We hope that the results from this study stimulate synthetic chemists to consider ways in which to synthesize the precursor compounds for further experimental investigations.

Supplementary Materials: The following supporting information can be downloaded at: <https://www.mdpi.com/article/10.3390/org4020016/s1>, GAMESS output files for all the propellanes, bicyclopentanes, and anionic bridgehead bromide optimizations. A video showing the optimization of anionic bridgehead bromide **12O** to form propellane **2O**.

Author Contributions: Conceptualization, G.W.B.; methodology, G.W.B.; validation, all authors; formal analysis, all authors; investigation, all authors; data curation, all authors; writing—original draft preparation, G.W.B.; writing—review and editing, all authors. All authors have read and agreed to the published version of the manuscript.

Funding: This research was funded by Berry College.

Data Availability Statement: Output files for all calculations are provided as Supplementary Materials.

Conflicts of Interest: The authors declare no conflict of interest. The funders had no role in the design of the study; in the collection, analyses, or interpretation of data; in the writing of the manuscript; or in the decision to publish the results.

References

1. Wiberg, K.B.; Walker, F.H. [1.1.1]Propellane. *J. Am. Chem. Soc.* **1982**, *104*, 5239–5240. [[CrossRef](#)]
2. Karadakov, P.B.; Stewart, B.; Cooper, D.L. Magnetic Shielding Analysis of Bonding in [1.1.1]Propellane. *J. Phys. Chem. A* **2023**, *127*, 861–869. [[CrossRef](#)] [[PubMed](#)]
3. Sterling, A.J.; Durr, A.B.; Smith, R.C.; Anderson, E.A.; Duarte, F. Rationalizing the Diverse Reactivity of [1.1.1]Propellane through σ - π -Delocalization. *Chem. Sci.* **2020**, *11*, 4895–4903. [[CrossRef](#)] [[PubMed](#)]
4. Jacobsen, H. The Local Kinetic Energy Profile of an Inverted Carbon–Carbon Bond Reveals and Refines its Charge-Shift Character. *ChemPhysChem* **2014**, *15*, 2522–2529. [[CrossRef](#)] [[PubMed](#)]
5. Gershoni-Poranne, R.; Stanger, A. An MO-Based Identification of Charge-Shift Bonds. *ChemPhysChem* **2012**, *13*, 2377–2381. [[CrossRef](#)]

6. He, F.-S.; Xie, S.; Yao, Y.; Wu, J. Recent Advances in the Applications of [1.1.1]-Propellane in Organic Synthesis. *Chin. Chem. Lett.* **2020**, *31*, 3065–3072. [[CrossRef](#)]
7. Dilmac, A.M.; Spuling, E.; de Meijere, A.; Brase, S. Propellanes—From a Chemical Curiosity to “Explosive” Materials and Natural Products. *Angew. Chem. Int. Ed.* **2017**, *56*, 5684–5718. [[CrossRef](#)]
8. Xu, H.; Saebø, S.; Pittman, C.U. A Coupled-Cluster Approach to the Relative Strains in [1.1.1]Propellane, its Derivatives and Hetero[1.1.1]propellanes. *Molec. Phys.* **2012**, *110*, 2349–2357. [[CrossRef](#)]
9. Ebrahimi, A.; Deyhimi, F.; Roohi, H. Natural Bond Order (NBO) Population Analysis of the Highly Strained Central Bond in [1.1.1]Propellane and Some [1.1.1]Heteropropellane Compounds. *J. Mol. Struct. Theochem* **2003**, *626*, 223–229. [[CrossRef](#)]
10. Zoller, U.; Chen, F.-P. In Pursuit of the Elusive Trithia [1.1.1]propellane: Synthesis of Potential 1,3-Dithietane Precursors. *Sulfur Lett.* **2002**, *25*, 115–121. [[CrossRef](#)]
11. Ebrahimi, A.; Deyhimi, F.; Roohi, H. Investigation of Structural Properties of Heteropropellane Compounds by ab initio Methods. *J. Chem. Res.* **2000**, *2000*, 93–95. [[CrossRef](#)]
12. Zoller, U.; Riggs, N.; Nguyen, M.T.; Radom, L. Trithia[1.1.1]propellane. *Phosphorus Sulfur Silicon Relat. Elem.* **1993**, *74*, 437–438. [[CrossRef](#)]
13. Riggs, N.V.; Zoller, U.; Nguyen, M.T.; Radom, L. Structure, Infrared and Raman Spectra, and Thermochemistry of Trithia[1.1.1]propellane. *J. Am. Chem. Soc.* **1992**, *114*, 4354–4356. [[CrossRef](#)]
14. Nguyen, K.A.; Carroll, M.T.; Gordon, M.S. Structures and Bonding of Group IV Sulfur and Oxygen Propellane Derivatives. *J. Am. Chem. Soc.* **1991**, *113*, 7924–7929. [[CrossRef](#)]
15. Grzonka, M.; Knop, J.V.; Klasinc, L.; Trinajstić, N. Theoretical Studies on Small Ring Heteropropellanes. *Oxapropellanes. Croatica Chem. Acta* **1984**, *57*, 1629–1632.
16. Weinges, K.; Klessing, K.; Kolb, R. Synthese und Spektroskopische Eigenschaften von Dithia- und Oxathia-Propellanen. *Chem. Ber.* **1973**, *106*, 2298–2304. [[CrossRef](#)]
17. Wiberg, K.B. Small-Ring Propellanes. *Chem. Rev.* **1989**, *89*, 975–983. [[CrossRef](#)]
18. Wiber, K.B.; Pratt, W.E.; Bailey, W.F. Reaction of 1,4-Diiodonorbomane, 1,4-Diiodobicyclo[2.2.2]octane, and 1,5-Diiodo[3.2.1]octane with Butyllithium. Convenient Preparative Routes to the [2.2.2]- and [3.2.1]Propellanes. *J. Am. Chem. Soc.* **1977**, *99*, 2297–2302. [[CrossRef](#)]
19. Alexander, P.J.; Button-Jennings, D.; Evans, C.N.; Hemstreet, M.B.; Henager, M.E.; Jacob, S.; Jolly, C.S.; Lantzman, M.R.; Saputo, A.; Stager, N.R.; et al. Introduction of a Computational Chemistry Course-Based Undergraduate Research Experience (CURE) into an Advanced Organic Chemistry Lab: An Investigation of Propellane Formation. *World J. Chem. Edu.* **2021**, *9*, 88–93. [[CrossRef](#)]
20. Wiberg, K.B.; Caringi, J.J.; Maturro, M.G. Kinetics of the Thermolysis of [*n*.2.2]Propellanes and Related Compounds. Mechanism of the Thermolysis of Bicyclo[2.2.0]hexanes. *J. Am. Chem. Soc.* **1990**, *112*, 5854–5861. [[CrossRef](#)]
21. Eaton, P.E.; Nyi, K. [4.2.2]- and [3.2.2]Propellanes. *J. Am. Chem. Soc.* **1971**, *93*, 2786–2788. [[CrossRef](#)]
22. Barca, G.M.J.; Bertoni, C.; Carrington, L.; Datta, D.; De Silva, N.; Deustua, J.E.; Fedorov, D.G.; Gour, J.R.; Gunina, A.O.; Guidez, E.; et al. Recent developments in the general atomic and molecular electronic structure system. *J. Chem. Phys.* **2020**, *152*, 154102. [[CrossRef](#)] [[PubMed](#)]
23. Mennuchi, B. Polarizable Continuum Model. *WIREs Comput. Mol. Sci.* **2012**, *2*, 386–404. [[CrossRef](#)]
24. Perri, M.J.; Weber, S.H. Web-Based Job Submission Interface for the GAMESS Computational Chemistry Program. *J. Chem. Ed.* **2014**, *91*, 2206–2208. [[CrossRef](#)]
25. Grimme, S. Density Functional Theory with London Dispersion Corrections. *WIREs Comput. Mol. Sci.* **2011**, *1*, 211–228. [[CrossRef](#)]
26. Kraemer, Y.; Ghiazza, C.; Ragan, A.N.; Ni, S.; Lutz, S.; Neumann, E.K.; Fetting, J.C.; Nöthling, N.; Goddard, R.; Cornella, J.; et al. Strain-Release Pentafluorosulfanylation and Tetrafluoro(aryl)sulfanylation of [1.1.1]Propellane: Reactivity and Structural Insights. *Angew. Chem. Int. Ed.* **2022**, *61*, e202211892. [[CrossRef](#)]
27. Wang, R.; Yang, S.; Li, Q. Coinage-Metal Bond Between [1.1.1]Propellane and M₂/MCl/MCH₃ (M = Cu, Ag, and Au): Cooperativity and Substituents. *Molecules* **2019**, *24*, 2601. [[CrossRef](#)]
28. Caputo, D.F.J.; Arroniz, C.; Durr, A.B.; Mousseau, J.J.; Stepan, A.F.; Mansfield, S.J.; Anderson, E.A. Synthesis and Applications of Highly Functionalized 1-Halo-3-Substituted Bicyclo[1.1.1]pentanes. *Chem. Sci.* **2018**, *9*, 5295–5300. [[CrossRef](#)]

Disclaimer/Publisher’s Note: The statements, opinions and data contained in all publications are solely those of the individual author(s) and contributor(s) and not of MDPI and/or the editor(s). MDPI and/or the editor(s) disclaim responsibility for any injury to people or property resulting from any ideas, methods, instructions or products referred to in the content.